RESEARCH PAPER

PCCP
www.rsc.org/pccp

Indium(III) hydration in aqueous solutions of perchlorate, nitrate and sulfate. Raman and infrared spectroscopic studies and *ab-initio* molecular orbital calculations of indium(III)–water clusters†‡

Wolfram W. Rudolph,*[a] Dieter Fischer,[b] Madelaine R. Tomney[c] and Cory C. Pye[c]

[a] *Medizinische Fakultät der TU Dresden, Institut für Virologie im MTZ, Fiedlerstr. 42, D-01307 Dresden, Germany. E-mail: Wolfram.Rudolph@mailbox.tu-dresden.de*
[b] *Institute of Polymer Research Dresden, Hohe Strasse 6, D-01069 Dresden, Germany*
[c] *Department of Chemistry, St. Mary's University, 923 Robie Street, Halifax, Nova Scotia, Canada B3H 3C3*

Received 17th May 2004, Accepted 24th August 2004
First published as an Advance Article on the web 21st September 2004

Raman and infrared spectra of aqueous In^{3+}-perchlorate, -nitrate and -sulfate solutions were measured as a function of concentration and temperature. Raman spectra of In^{3+} perchlorate solutions reveal a strongly polarized mode of medium to strong intensity at 487 cm^{-1} and two broad, depolarized modes at 420 cm^{-1} and 306 cm^{-1} of much lesser intensity. These modes have been assigned to $\nu_1(a_{1g})$, $\nu_2(e_g)$ and $\nu_5(f_{2g})$ of the hexaaquaindium(III) ion, $[In(OH_2)_6{}^{3+}]$ (O_h symmetry), respectively. The infrared active mode at 472 cm^{-1} has been assigned to $\nu_3(f_{1u})$. The Raman spectra suggest that $[In(OH_2)_6{}^{3+}]$ is stable in acidified perchlorate solutions, with no inner-sphere complex formation or hydroxo species formed over the concentration range measured. In concentrated $In(NO_3)_3$ solutions, In^{3+} can exist in form of both an inner-sphere complex, $[In(OH_2)_5ONO_2]^{2+}$ and an outer-sphere complex $[In(OH_2)_6{}^{3+} \cdot NO_3{}^-]$. Upon dilution the inner-sphere complex dissociates and the amount of the outer-sphere complex increases. In dilute solutions the cation, $[In(OH_2)_6{}^{3+}]$, exists together with free nitrate. In indium sulfate solutions, a stable In^{3+} sulfato complex could be detected using Raman spectroscopy and 115-In NMR. Sulfato complex formation is favoured with increase in temperature and thus is entropically driven. At temperatures above 100 °C a basic In^{3+} sulfate, $In(OH)SO_4$ is precipitated and characterised by wet chemical analysis and X-ray diffraction. *Ab initio* geometry optimizations and frequency calculations of $[In(OH_2)_n{}^{3+}]$ clusters (n = 1–6) were carried out at the Hartree–Fock and second order Møller–Plesset levels of theory, using various basis sets up to 6-31+G*. The global minimum structure of the aqua In^{3+} species was reported. The unscaled vibrational frequencies of the $[In(OH_2)_6{}^{3+}]$ cluster do not correspond well with experimental values because of the missing second hydration sphere. The theoretical binding enthalpy for $[In(OH_2)_6{}^{3+}]$ accounts for *ca.* 60% of the experimental single ion hydration enthalpy for In^{3+}. Calculations are reported for the $[In(OH_2)_{18}{}^{3+}]$ cluster (In[6 + 12]) with two full hydration spheres (T symmetry), for which the calculated $\nu_1(InO_6)$ mode occurs at 483 cm^{-1} (HF/6-31G*), which is in good agreement with the experimental value at 487 cm^{-1}, as are the other frequencies. The theoretical binding enthalpy for $[In(OH_2)_{18}{}^{3+}]$ was calculated and underestimates by about 15% the experimental single ion hydration enthalpy of In^{3+}.

1 Introduction

Recently, we have studied the vibrational spectra of some trivalent hexaaqua cations (Al^{3+},[1] Ga^{3+},[2] Sc^{3+} [3,4]). In addition, *ab initio* molecular orbital calculations have been carried out to determine their vibrational spectra in order to verify the spectroscopic results.[5] In this paper we extend our studies to the hexaaqua cation In^{3+} in order to contribute to the understanding of indium speciation.[5]

Industrial uses of indium include the low melting alloys with Cd, Zn, Cu, Pb, and Bi (melting point 50–100 °C) used in security switches, thermostats and for soldering. Its main use is in the semiconductor industry as a component of $A^{III}B^{V}$ compounds (InP, InAs and InSb).[6] The solid state chemistry of indium is quite well studied. On the other hand, the aqueous solution chemistry of In^{3+} has not drawn much attention.

Indium speciation is complex. Firstly, indium species easily hydrolyze to form both mono- and polynuclear hydroxo species such as $[InOH]^{2+}$, $In_2(OH)_2{}^{4+}$ [7] and $In_4(OH)_6{}^{6+}$.[8] In so-called basic or under-stoichiometric solutions (solutions with an OH/In ratio >0), polynuclear hydroxo complexes could be identified.[8,9] In an earlier potentiometric investigation of the hydrolysis of the In^{3+} ion in aqueous perchlorate solution, the data were explained by the formation of the mononuclear complexes $InOH^{2+}$ and $In(OH)_2{}^+$ and an infinite series of polynuclear complexes, $In[(OH)_2In]_n{}^{(3+n)+}$.[9] Large angle X-ray scattering measurements on hydrolyzed In^{3+} nitrate solution showed the presence of polynuclear hydrolysis complexes with In–In distances of 3.89 Å, indicating single hydroxo bridges between the In atoms. The data are consistent with a dominant four-nuclear complex, $In_4(OH)_6{}^{6+}$.[8]

Secondly, stable complexes with most common anions can be observed. In aqueous $InCl_3$ and $InBr_3$ solutions for instance, stable In^{3+}-chloro or -bromo complexes $[InX_n(OH_2)_{6-n}]^{(3-n)+}$ are formed,[10–12] although there is some dispute about the exact nature of these species.[13]

† A preliminary account of this and other work has been published (see ref. 55).

‡ Electronic supplementary information (ESI) available: Spectroscopic data for In(III)-nitrate and In(III)-sulfate solutions (Tables S1–S7); the O–H bond length and the H–O–H angle of the first sphere waters in In(III)–water clusters as a function of the coordination number (Figs. S1 and S2). See http://www.rsc.org/suppdata/cp/b4/b407419j/

DOI: 10.1039/b407419j

The hydrolysis and complex formation prevent easy characterization of the hexaaquaindium(III) ion and so it is not surprising that the hydration structure of In(III) has only recently been determined (*cf.* ref. 14). A combined large angle X-ray scattering and EXAFS study shed light on the nature of the first and second hydration shells of In^{3+} in aqueous $In(ClO_4)_3$ solutions.[15]

In this paper we present Raman, infrared and 115-In NMR results on aqueous $In(ClO_4)_3$, $In(NO_3)_3$, and $In_2(SO_4)_3$ solutions under acidic conditions in order to characterize the hexaaquaindium(III). Perchlorate was chosen because as a weak Lewis base it is unlikely to penetrate the first hydration sphere of In^{3+}. A slight excess of acid has been used to prevent hydrolysis. Nitrate and sulfate solutions were selected because they show the effects of increased association.

Additionally, *ab initio* molecular orbital calculations of In^{3+}–water clusters modelling the inner-sphere, denoted as In[n + 0], with n equal to 1–6 are presented. The cluster $[In(OH_2)_6{}^{3+}]$ constitutes the species with the full first coordination sphere (denoted In[6 + 0]). A cluster with the complete inner-sphere and an outer-sphere of twelve water molecules (In[6 + 12]) has also been modelled and included in our discussion. The main aim of these *ab initio* calculations has been to verify the vibrational modes of the InO_6 unit. Calculations on indium(III) aqua complexes with either nitrate or sulfate are more complex and will be considered in a future publication.

2 Experimental details and data analysis

$In(ClO_4)_3$ solutions were prepared by dissolving In_2O_3 with a stoichiometric amount of $HClO_4$. Three solutions were prepared: solution (A) was 1.650 mol l^{-1} $In(ClO_4)_3$ with a slight excess of perchloric acid (*ca.* 0.015 mol/l) , solution (B) was 1.246 mol l^{-1} $In(ClO_4)_3$ with 0.05 mol l^{-1} $HClO_4$ excess, and solution (C) was 1.105 mol l^{-1} $In(ClO_4)_3$ with 1.310 mol l^{-1} $HClO_4$ in excess.

An $In(NO_3)_3$ stock solution 2.800 mol l^{-1} (3.725 mol kg^{-1}) was prepared by dissolving In_2O_3 with a stoichiometric amount of HNO_3 and in addition a slight excess of HNO_3 (approximately 0.1 mol) was added to the stock solutions to prevent hydrolysis. A further three solutions were prepared by weight: 1.117 mol l^{-1} (1.213 mol kg^{-1}); 0.534 mol l^{-1} (0.561 mol kg^{-1}); and 0.312 mol l^{-1} (0.320 mol kg^{-1}).

A 1.659 mol l^{-1} $In_2(SO_4)_3$ stock solution (1.976 mol kg^{-1}) was prepared by dissolving In_2O_3 with sulfuric acid. A total of 5 solutions including the stock solution were prepared by weight: 1.659 mol l^{-1} (1.976 mol kg^{-1}); 0.627 mol l^{-1} (0.657 mol kg^{-1}); 0.237 mol l^{-1} (0.241 mol kg^{-1}); 0.0986 mol l^{-1} (0.0994 mol kg^{-1}); and 0.0329 mol l^{-1} (0.0330 mol kg^{-1}). The In(III) content of the solutions was determined complexometrically with xylenol orange as indicator.[16] Solution densities were determined with a pycnometer (5 ml) at 25 °C.

CsIn alum, $CsIn(SO_4)_2 \cdot 12H_2O$, was prepared by standard procedures and re-crystallized twice from its aqueous solution.[17]

Raman spectra were measured with equipment at the TU Freiberg Mining Academy. The spectra were excited with a 514.5 nm line of an Ar^+ laser at power levels ranging from 0.8 to 1.2 W. After passing the Zeiss double monochromator GDM 1000, with gratings with 1300 grooves per mm, the scattered light was detected with a cooled photo multiplier tube ITT 130 in the photon counting mode. A scrambler before the slit served to compensate for grating preference. I_{VV} and I_{VH} spectra were obtained with fixed polarisation of the laser beam by rotating the polarisor at 90° between the sample and the entrance slit to give the scattering geometries:

$$I_{VV} = I(Y[ZZ]X) = 45\alpha'^2 + 4\gamma'^2 \quad (1)$$

$$I_{VH} = I(Y[ZY]X) = 3\gamma'^2 \quad (2)$$

The isotropic spectrum, I_{iso} or I_α is then constructed:

$$I_{iso} = I_{VV} - 4/3 \cdot I_{VH}. \quad (3)$$

In order to get spectra defined as $I(\bar{\nu})$ which are independent of the excitation frequency ν_L, the measured Stokes intensity should be corrected for the scattering factor $(\nu_L - (\bar{\nu}))$.[4] In the case of counting methods used, the measured count rates have to be corrected with the factor $(\nu_L - (\bar{\nu}))$.[3] The spectra were further corrected for the Bose–Einstein temperature factor, $B = [1 - \exp(-h\bar{\nu}c/kT]$, and the frequency factor, $\bar{\nu}$, to give the so called reduced or $R_Q(\bar{\nu})$ spectrum, which is directly proportional to the point-by-point relative scattering activity, $S_Q(\bar{\nu})$, in terms of mass-weighted normal coordinates, Q, in the double harmonic approximation. $R_Q(\bar{\nu})$ is the form of the Raman spectrum that most closely approaches the vibrational density of states.[18] The relationship between the $I(\bar{\nu})$ and $R_Q(\bar{\nu})$ forms of the spectra is given by eqn. (4).

$$S_Q(\bar{\nu}) \propto R_Q(\bar{\nu}) = I(\bar{\nu}) \cdot \bar{\nu} \cdot B \quad (4)$$

The normalized isotropic R-spectra were constructed by subtraction:

$$R_Q(\bar{\nu})_{iso} = R_Q(\bar{\nu})_{VV} - 4/3R_Q(\bar{\nu})_{VH} \quad (5)$$

In the low frequency region the $I(\bar{\nu})$ and $R_Q(\bar{\nu})$ spectra are significantly different and only the R-format spectra are presented. It should be noted that one of the advantages of using isotropic spectra is that the baseline is almost flat in the 50–700 cm^{-1} frequency region allowing relatively unperturbed observation of any weak modes present.

For quantitative measurements, the perchlorate band, ν_1-ClO_4^- at 935 cm^{-1} was used as an internal standard. The relative isotropic scattering coefficient $S(\nu_1\text{-}InO_6)$ was obtained from the R_{iso} spectra. The advantage of S values over J values is that S values can be put on an absolute scale.[19] Further spectroscopic details about the high temperature measurements, the band fit procedure and the procedure about R normalized Raman spectra are given in previous publications.[20]

The solution spectra were measured with the FT-IR spectrometer IFS66v (BRUKER OPTICS, Germany) applying an ATR-Overhead accessory (SPECAC, UK) with a diamond crystal in the wavelength range from 600 to 4000 cm^{-1} with a spectral resolution of 2 cm^{-1}.

The solid, $CsIn(SO_4)_2 \cdot 12\ H_2O$, was measured in nujol between KBr discs, which where coated with polyethylene films with the FT-IR spectrometer IFS66v (BRUKER OPTICS, Germany) employing a Mylar beamsplitter. The spectral resolution was 4 cm^{-1}. 50 scans were taken in the wavelength range from 100 to 4000 cm^{-1}. All measurements were carried out at 23 °C.

Variable temperature 115-In NMR spectra were obtained with a General Electric NMR spectrometer GN-300, operating at 66.097 MHz, using a 10 mm broad band probe and working with an external lock. A 1.00 M $In(NO_3)_3$ solution in D_2O was used as a reference and the signal was set at 0 ppm. Sixteen spectra were usually accumulated. The data were processed with the software package NUTS from NMR Data Processing Software, Fremont, Ca.

Ab initio calculations with the STO-3G,[21] 3-21G,[22] and 6-31G*[23] basis sets were employed. Gaussian 92 was used for most calculations.[24] Huzinaga's (433321/43321/431*) basis set was used for indium in conjunction with the 6-31G* water basis set.[25] All structures were confirmed to be a local minimum (unless otherwise indicated) by analytic frequency evaluation. A diffuse sp-shell was added to the oxygen atoms to give the standard 6-31+G* basis. Møller-Plesset perturbation theory (with frozen cores) was used to approximate correlation effects (as MP2/6-31G* and MP2/6-31+G*). For the octadecaaquaindium(III) ion, the level of theory was restricted to the Hartree–Fock.

In addition to the above calculations, some geometry optimizations and analytical frequency calculations were carried out with Gaussian 98[26a] using some built-in effective core potential basis sets and pseudopotentials.[26b]

3 Results and discussion

3.1 General remarks

Both 1-H- and 115-In NMR have been employed to confirm the presence of $[In(OH_2)_6^{3+}]$ in aqueous perchloric acid solution.[27] XRD studies in an aqueous solution of 1.7 M In(III)(aq.) quote the In–O bond length as 2.15 Å.[28] A recent combined EXAFS and LAXS study,[15] quoting a mean value for the In–O bond length as 2.121(2) Å in aqueous solution, confirms the older data. This value is significantly shorter than the sum of the effective size of In(III) and H_2O. The existence of the $[In(OH_2)_6^{3+}]$ cation has also been confirmed in the solid state, in cesium indium alums.[28] Aqueous indium(III) solutions are very acidic and a wide range of $-\log Q_{11}$ values (formation of $In(OH)^{2+}$(aq.)) have been quoted, ranging from 3.7 to 4.4.[9,29] A pK_{11} value of 4.31 at 25 °C at zero ionic strength has been reported more recently by Sylva and co-workers.[9] Rapid water exchange of the water molecules of the first hydration sphere with the bulk water has been measured recently: $k_1 \geq 1 \times 10^7$ s^{-1} at 25 °C.[30] The exchange mechanism of the water at In_{aq} is **A** compared to the **D** mechanism at $Al_{aq.}$ and Ga_{aq}.[30] The aqua indium(III) cation has a somewhat labile first hydration sphere. With favorable thermodynamics, most common anions can easily exchange with water in the first coordination sphere of this d^{10} cation (except perchlorate).[30]

3.2 Spectroscopic considerations on the $In(OH_2)_6^{3+}$ ion

The $In(OH_2)_6^{3+}$ ion (in the gas phase) possesses T_h symmetry (see Fig. 1) and its 19 atoms give rise to 3N-6 = 51 normal modes (n.m.).[31–33] The irreducible representation is as follows:

$$\Gamma_v(T_h) = 3a_g(\text{Ra, t.p.}) + a_u(\text{n.a.}) + 3e_g(\text{Ra, dp}) + e_u(\text{n.a.}) + 5f_g(\text{Ra, dp}) + 8f_u.(\text{IR}). \quad (6)$$

The InO_6 subunit possesses O_h symmetry. For the 15 n.m. the irreducible representation is:

$$\Gamma_v(O_h) = a_{1g}(\text{Ra, t.p.}) + e_g(\text{Ra, dp}) + 2f_{1u}(\text{i.r.}) + f_{2g}(\text{Ra, dp}) + f_{2u}(\text{n.a.}) \quad (7)$$

Due to the mutual exclusion rule, the Raman active modes are infrared forbidden and *vice versa*.

3.3 Vibrational spectroscopic results of $In(ClO_4)_3$ solutions

The $In(ClO_4)_3$ solution spectra reveal the Raman modes for both the perchlorate anion, discussed first, and the InO_6 unit of the $[In(OH_2)_6^{3+}]$ species, as shown in the overview spectrum (see Fig. 2).

3.3.1 The ClO_4^- modes. The ClO_4^- ion possesses T_d-symmetry and the nine modes of internal vibrations ($\Gamma_{vib}(T_d) =$ a_1(Ra, t.p.) + e(Ra, dp) + $2f_2$(Ra, dp, i.r.)) have been described in detail.[34] The spectrum of an $In(ClO_4)_3$ solution shows the predicted four Raman-active bands for the tetrahedral ClO_4^-. The $\nu_1(a_1)$ ClO_4^- mode centred at 935 cm^{-1} is totally polarised ($\rho = 0.003$), whereas $\nu_3(f_2)$ ClO_4^- centred at 1112 cm^{-1} is depolarised, as are the deformation modes $\nu_4(f_2)$ ClO_4^- at 630 cm^{-1} and $\nu_2(e)$ ClO_4^- at 463 cm^{-1}. In infrared only the f modes are active, namely ν_3-ClO_4 at 1112 cm^{-1}, and ν_4-ClO_4^- at 630 cm^{-1} (Fig. 2, top spectrum). The $\nu_1(a_1)$ ClO_4^- mode, formally infrared-forbidden, shows as an extremely weak mode at 935 cm^{-1}.

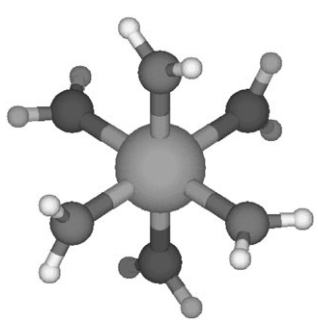

Fig. 1 Structural model of $In(OH_2)_6^{3+}$ (symmetry T_h).

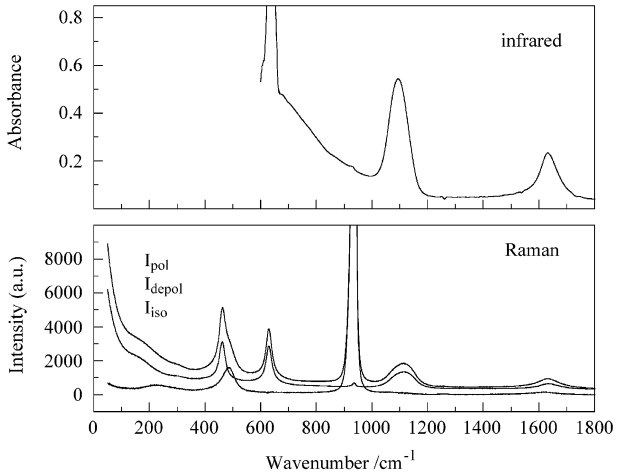

Fig. 2 Overview spectra: Infrared (top) and Raman spectrum, I_{pol}, I_{depol}, and I_{iso} scattering (bottom) of a 1.246 mol l^{-1} $In(ClO_4)_3$ plus 0.05 mol l^{-1} $HClO_4$ solution at 23 °C in the frequency range from 50 to 1800 cm^{-1}. Note that the infrared spectrum starts from 600 cm^{-1}.

3.3.2 The InO_6 modes. Raman spectra of $In(ClO_4)_3$ solutions show all three predicted Raman-active InO_6 modes. As their positions do not coincide with the i.r. active mode(s) it may be concluded that the $[In(OH_2)_6^{3+}]$ species is centrosymmetric. The strongly polarized $\nu_1(a_{1g})$ InO_6 mode at 487 ± 1 cm^{-1} (Fig. 3a) is independent of the acidity and perchlorate concentration. This indicates the absence of hydroxo complexes and of penetration of ClO_4^- into the coordination sphere of $[In(OH_2)_6]^{3+}$. The full width at half maximum height (fwhh) in solution A (61 cm^{-1}) is slightly larger than in solutions B and C (55 cm^{-1}).

Earlier reports on aqueous indium(III) perchlorate solutions quoted much lower values for $\nu_1(InO_6)$: 400 [14c] and 420 cm^{-1},[35] but only the isotropic spectrum allows undisturbed detection of the $\nu_1(InO_6)$ mode. This is because in the polarised spectrum, $\nu_2(e)$ ClO_4^- at 464 cm^{-1} partially overlaps ν_1 and leads to an incorrect peak position (see Fig. 3a). Values of 475 cm^{-1} [36] and 485 cm^{-1} [37]) given recently for $\nu_1(InO_6)$ from spectra of nitrate solutions are also incorrect because, as will be shown below, nitrate penetrates the first coordination sphere of In^{3+} and shifts the ν_1 peak position to lower frequencies.

In the solid caesium alum, $CsIn(SO_4)_2 \cdot 12H_2O$, the $\nu_1(InO_6)$ mode occurs at slightly higher frequencies, namely at 492 cm^{-1} at 296 K. This mode is strongly temperature dependent and shifts to 505 cm^{-1} at 80 K, due to the strong hydrogen bonds in the Cs alum.[17,38] This is also true for the other modes and must be kept in mind if one wants to compare the results from solid state Raman spectroscopy at 77 K with the results for aqueous In^{3+} solutions at 298 K. For other metal ions the solution frequency values are equal or a bit smaller than the solid state values.[1–3,17] The static hydrogen bonds in a solid may be stronger than the dynamic hydrogen bonds in a liquid. The fact that at room temperature the $\nu_1(InO_6)$ mode in the CsIn alum and the aqueous solutions are comparable allows us to take the ν_3 InO_6 frequency from the CsIn alum infrared

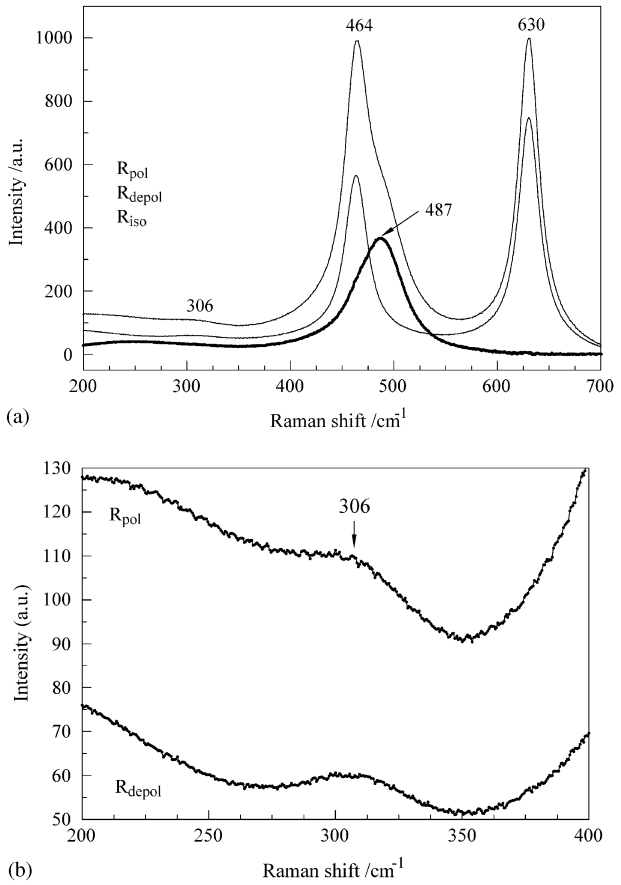

Fig. 3 (a) Raman spectrum, R_{pol}, R_{depol}, and R_{iso} scattering of a 1.246 mol l^{-1} $In(ClO_4)_3$ plus 0.05 mol l^{-1} $HClO_4$ solution at 23 °C in the frequency range from 200 to 700 cm^{-1}. (b) Raman spectrum, R_{pol}, and R_{depol} scattering of a 1.246 mol l^{-1} $In(ClO_4)_3$ plus 0.05 mol l^{-1} $HClO_4$ solution at 23 °C in the frequency range from 200 to 400 cm^{-1}. The broad mode at 306 cm^{-1} represents the $\nu_5(InO_6)$ mode of the InO_6 skeleton.

spectra. In the infrared spectrum of CsIn alum at room temperature the $\nu_3(f_{1u})$ InO_6 mode is assigned to 472 cm^{-1} significantly distinct from the Raman active mode, $\nu_1(a_{1g})InO_6$ at 487 cm^{-1}.

In the depolarized Raman spectrum a mode at 306 ± 2 cm^{-1} (see Fig. 3b) is assigned to $\nu_5(f_{2g})$. The weak mode at *ca.* 420 ± 5 cm^{-1} is obscured by the strong ν_2(e) ClO_4^- mode at 464 cm^{-1} but can be observed in dilute $In(NO_3)_3$ solutions (see below). The i.r. active mode $\nu_3(f_{1u})$ was observed at 472 cm^{-1}, while the second i.r. active mode could not be observed. The assignment of the InO_6 modes together with the values of $[In(OH_2)_6^{3+}]$ in solution (our values), and in caesium alum[17] are given in Table 1. Upon deuteration the InO_6 mode of the $[(In(OD_2)_6^{3+}]$ species shifts by the factor of 0.949 and values for ν_1 InO_6 and ν_5 InO_6 of $In(ClO_4)_3$ in D_2O are also given in Table 1.

Mink *et al.*[39] in a recent paper assigned not only ν_1 InO_6 = 475 cm^{-1} but also ν_2 InO_6 = 401 cm^{-1} and ν_5 InO_6 = 145 cm^{-1} which are significantly different from our Raman values (*cf.* our Raman data in Table 1). Together with their infrared data (*cf.* Table 3 in ref. 39) they postulated that the indium(III) hexaaqua complex should possess T_h symmetry. Critically evaluating their experimental values leads us to the conclusion that these data and their subsequent assignments seem doubtful.

Hydrolysis effect: In both solutions, B (4% excess $HClO_4$) and C (120% excess $HClO_4$) the fwhh remains the same at 54 cm^{-1}. In these acidic solutions the hydrolysis is negligible. In solution A (1% excess $HClO_4$) the fwhh is only slightly bigger (10–12%). This is clear proof that the hydrolysis does not affect the $\nu_1(a_{1g})$ InO_6 modes unless only a slight excess of $HClO_4$ is present.

Temperature effect on $\nu_1(InO_6)$: The position of the symmetric stretching mode of $[In(OH_2)_6^{3+}]$, $\nu_1(a_{1g})$ InO_6, for solution (B) is virtually unchanged at 486 ± 1 cm^{-1} between 25 and 75 °C. However, the fwhh increases from 55 cm^{-1} (at 25 °C), to 60 cm^{-1} (at 50 °C), to 68 cm^{-1} (at 75 °C), whilst the symmetry of the band profile persists. The latter is consistent with perchlorate not penetrating into the inner sphere of the $[In(OH_2)_6^{3+}]$. The broadening is possibly due to the strong interactions between the first and second hydration shells or perhaps between cations in this relatively concentrated solution.

Comparison with other trivalent cations: It is noteworthy that the group 13 $[M(OH_2)_6^{3+}]$ ions do not follow the relation $\nu_1 \propto 1/(r_{M-O})^2$ as also reported by Kanno,[36] derived from the Born model since: $\nu_1(AlO_6)$ = 525 cm^{-1},[1] $\nu_1(GaO_6)$ = 526 cm^{-1},[2,40] $\nu_1(InO_6)$ = 487 cm^{-1} [this work] and $\nu_1(TlO_6)$ = 450 cm^{-1}.[41] The simple Born model, although useful in many situations, is not appropriate in this case, as it demands a more rigorous treatment as shown below. In^{3+} is a much softer cation than Al^{3+} or Ga^{3+} and this is reflected by its scattering intensity. The relative molar scattering intensities, S_h for the symmetric stretching modes ν_1 MO_6 (M = In^{3+}, Ga^{3+}, and Al^{3+}) of the group 13 metal ions follows the order: $S_h(In^{3+})$ = 0.22 [this work] > $S_h(Ga^{3+})$ = 0.14[2] > $S_h(Al^{3+})$ = 0.033.[1]

A very weak and broad mode centred on 190 ± 10 cm^{-1} can also be observed in $In(ClO_4)_3$ solutions (Fig. 2). This mode may also be observed in pure water (centred around 195 cm^{-1}), for which it is moderately intense but slightly polarized. It has been assigned to a restricted translational mode of H-bonded water molecules. This mode is strongly anion and concentration dependent.[14d]

Table 1 The Raman and infrared data (frequencies and fwhh in cm^{-1}, and band intensities) on InO_6 skeleton modes (InO_6 possess O_h symmetry) from aqueous $In(ClO_4)_3$, and dilute $In(NO_3)_3$ solutions. (In $In(ClO_4)_3$ solutions the intensive ClO_4^- mode at 461 cm^{-1} overlaps $\nu_2(e_g)InO_6$). Additionally, the InO_{6-} modes from crystalline $CsIn(SO_4)_2 \cdot 12H_2O$ (space group *Pa*3 (T_h^6) (z = 4)) are given

			$CsIn(SO_4)_2 \cdot 12H_2O$	
Assignments and activities of InO_6	Exper.[a] frequencies in H_2O	Exper.[a] frequencies in D_2O	Our data (296 K)	From Ref. 17 (80 K)
$\nu_1(a_{1g})$ Ra	487 ± 1, (0.005) $\Gamma_{1/2}$ = 54, s	463 ± 2, (0.005) $\Gamma_{1/2}$ = 52	492	505
$\nu_2(e_g)$ Ra	420 ± 5 (0.75) $\Gamma_{1/2}$ = 60, vw	—	426, 430	425 (E_g), 430 (F_g), 458 (F_g), 468 (E_g), 476 (F_g)
$\nu_3(f_{1u})$ i.r.	472 ± 2	—		—
$\nu_4(f_{1u})$ i.r.	n.o.	—		—
$\nu_5(f_{2g})$ Ra	306 ± 4, (0.75) $\Gamma_{1/2}$ = 58, w	285 ± 2, (0.75)	286, 296, 308	291 (F_g), 297 (E_g), 298 (F_g), 322 (F_g)
$\nu_6(f_{2u})$ -	n.a.	n.a.	—	—

[a] Depolarization ratio in brackets; underneath $\Gamma_{1/2}$, the fwhh and intensity (s = strong, w = weak, vw = very weak); n.o. = mode not observed, n.a. = not active

The feature at 3560 cm^{-1} in the Raman spectrum of solution B (see Fig. 4) represents the stretching mode of OH weakly hydrogen bonded to the perchlorate anion: $O_3ClO^-\cdots H–O–H$. The broad shoulder at 2900 cm^{-1} in Fig. 4 reveals the OH stretching mode of the water molecules in the first hydration shell of $[In(OH_2)_6]^{3+}$. This is quite distinct from the OH stretching modes of bulk water at 3255 and 3385 cm^{-1}. Weak broad modes at 2045 and 2480 cm^{-1} may be assigned as combination modes of a librational mode with the deformation mode. A similar OH stretching profile was observed in $Al(ClO_4)_3$ solutions.[32]

To summarize, our Raman spectroscopic data on $In(ClO_4)_3$ solutions reveal that under the conditions studied, the hexaaquaindium(III) complex remains stable and no ion-pairing or hydrolysis takes place. However, we shall see below that the vibration spectra of $In(NO_3)_3$ and $In_2(SO_4)_3$ solutions reveal evidence of water ligand exchange, namely, differentiation of the ligated and non-ligated anion modes, a shift and/or splitting of the metal aqua modes, and the appearance of a metal–ligand mode at low frequencies.

3.4 Vibrational spectra of $In(NO_3)_3$ solutions

Overview infrared and Raman spectra of a 2.800 mol l^{-1} $In(NO_3)_3$ solution (R_w = mole ratio H_2O : $In(NO_3)_3$ = 15 : 1) from 700 to 1800 cm^{-1} are presented in Fig. 5. In addition, the Raman spectrum from 100 to 800 cm^{-1} is presented in Fig. 6a and from 1200 to 1800 cm^{-1} in Fig. 6b. The Raman and infrared data of aqueous $In(NO_3)_3$ solutions as a function of concentration are presented in Tables S1 and S2 respectively.‡ In aqueous $In(NO_3)_3$ solutions, vibrational modes of the In(III) aqua ions are observed in addition to the modes of the NO_3^- anion.

The "free" NO_3^- anion has D_{3h} symmetry and should exhibit a four-band spectrum: $\nu_1(a_1') = 1048$ cm^{-1}, Raman active only; $\nu_2(a_2'') = 830$ cm^{-1}, infrared active only; $\nu_3(e') = 1380$ cm^{-1}, Raman- and infrared active; $\nu_4(e') = 717$ cm^{-1}, Raman- and infrared active. However, in dilute aqueous solution, the vibrational spectra of alkali metal nitrates indicate the appearance of forbidden modes and doubling of the $\nu_3(e')$ mode, with broad depolarized components at 1348 and 1406 cm^{-1} (Raman) and 1347 and 1395 cm^{-1} (infrared).[42,43] It seems unlikely that the doublet structure is due to ion-pair formation, since the doublet has been found to be insensitive to both the nature of the cation and further dilution ($\leq$0.5 mol l^{-1}).[42–44] A specific $NO_3^-\cdots H_2O$ hydrogen-bonded species has been proposed.[43,44] The formation of inner-sphere species results in more pronounced alterations in the nitrate spectrum.

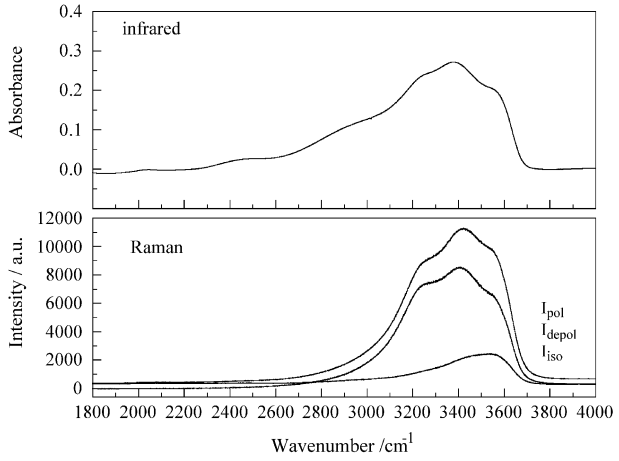

Fig. 4 Overview spectra: Infrared (top) and Raman spectrum, I_{pol}, I_{depol}, and I_{iso} scattering (bottom) of a 1.246 mol/l $In(ClO_4)_3$ plus 0.05 mol l^{-1} $HClO_4$ solution at 23 °C in the frequency range from 1800 to 4000 cm^{-1}.

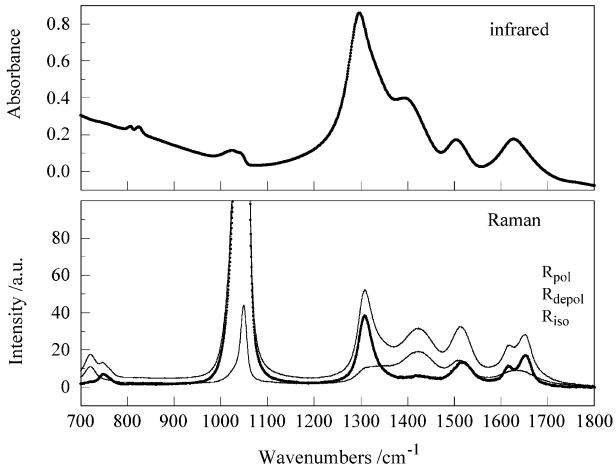

Fig. 5 Overview spectra of a 2.800 mol l^{-1} $In(NO_3)_3$ solution at 23 °C: Infrared (top) and Raman spectrum, R_{pol}, R_{depol}, and R_{iso} scattering, (bottom) in the frequency range from 700 to 1800 cm^{-1}.

Thus, for the $M^+\cdot ONO_2^-$ ion pair the Raman band positions can be summarized: 740 cm^{-1} (dp), 830 cm^{-1}, 1040–1060 cm^{-1} (p), 1320–1450 cm^{-1} (dp). The shift of $\nu_1(InO_6)$ from 487 cm^{-1} (unperturbed mode in perchlorate solution) to 475 cm^{-1} in the nitrate stock solution (2.800 mol l^{-1}) and the broad shoulder at 410 cm^{-1} of the mode reflects the presence of NO_3^- in the inner-coordination sphere.

Furthermore, upon dilution the isotropic mode $\nu_1(InO_6)$ shifts from 475 cm^{-1} (fwhh = 70 cm^{-1}) in a 2.80 mol l^{-1} solution (R_w = 15 : 1) to 484 cm^{-1} (fwhh = 66 cm^{-1}) in a

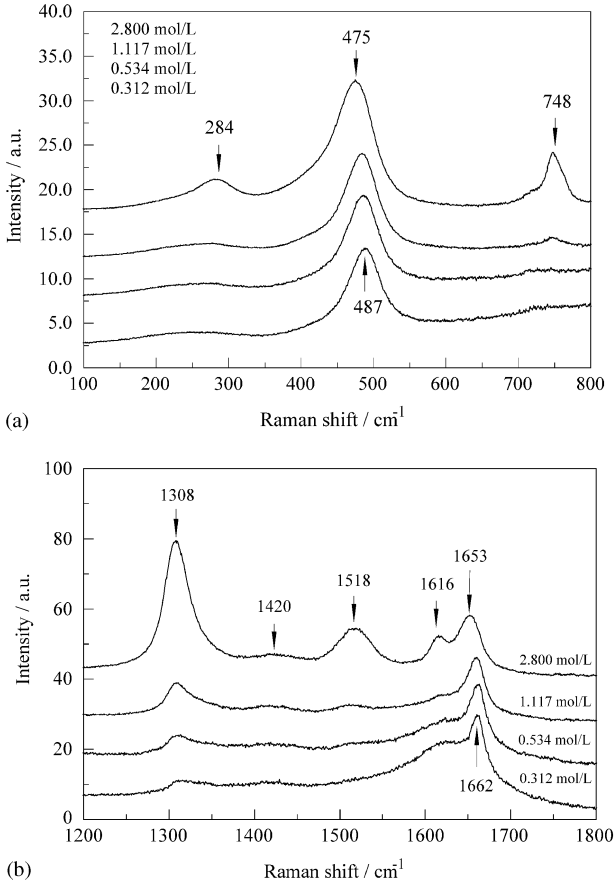

Fig. 6 (a) Concentration profile (isotropic Raman spectra (R_{iso})) of four aqueous $In(NO_3)_3$ solutions (concentrations in mol/l as indicated) from 100 to 800 cm^{-1} at 23 °C. (b) Concentration profile (isotropic Raman spectra (R_{iso})) of four aqueous $In(NO_3)_3$ solutions (concentrations in mol/l as indicated) from 1200 to 1800 cm^{-1} at 23 °C.

1.117 mol l^{-1} ($R_w = 46:1$) and to 487 cm^{-1} (53 cm^{-1}) in a 0.312 mol l^{-1} ($R_w = 173:1$) solution. The concentration profile of the isotropic Raman spectra of the four $In(NO_3)_3$ solutions (Fig. 6) demonstrates that upon dilution the inner-sphere complex disappears. The isotropic mode at 284 cm^{-1} (Fig. 6a) is another clear indication of the presence of an indium–nitrato complex, $[In(OH_2)_5ONO_2]^{2+}$ of likely C_{2v} symmetry.

Raman spectroscopic data of the stock solution show the following features for NO_3^-: 720 cm^{-1} (dp); 748 cm^{-1} (p), 762 cm^{-1} (shoulder), 806 and 828 cm^{-1}; 1048.5 cm^{-1} (p, depolarization ratio = 0.049) with shoulder at 1030 cm^{-1} and modes in the ν_4 region at 1308 cm^{-1} (p), 1420 (dp), 1518 (p) and the overtone $2\nu_2$ (a_1') at 1616 cm^{-1} (p) and 1653 cm^{-1} (p). The overtone at 1653 cm^{-1} overlaps with the deformation mode of water, ν_2(HOH), at 1646 cm^{-1}. Due to the big difference in the polarization ratios $2\nu_2$ (a_1') NO_3^- and ν_2 (HOH) the overtone $2\nu_2$ appears in the polarized scattering contribution beside the deformation mode of water. In the anisotropic scattering the weakly polarized mode ν_2(HOH) appears almost free from the contribution of the overtone. These features are depicted in Fig. 6b.

In the free ion approximation the mode ν_2 is Raman forbidden, therefore its activity can be taken as a measure of the strength of the interaction with the cation. For instance, in molten $CsNO_3$, KNO_3, and $NaNO_3$ the peak is barely detectable whereas it is easily observed in the Raman spectra of $LiNO_3$ and $AgNO_3$. The mode ν_2 is a non-degenerate i.r. active out-of-plane bending mode, therefore the appearance of a doublet structure indicates the presence of two non-equivalent sites. In aqueous solutions the variation of the two peaks assigned to ion-pairs and free-ions has been used to measure stability constants.[14c] The Raman overtone region ($2\nu_2$ *ca.* 1656 cm^{-1}, $\rho = 0.5$) is also a useful region to study because it is much more intense than the fundamental. Two modes have been observed in this region, namely at 1616 cm^{-1} and 1653 cm^{-1}, which also indicates the existence of the two nitrate forms, bound and "free" nitrate.

The shift and the structure of the $\nu_1(InO_6)$ mode (peak maximum at 475 cm^{-1}, broad shoulder at *ca.* 410 cm^{-1}), the isotropic contribution at 1315 cm^{-1} and the ligand mode, In^{3+}-ONO_2^- at 284 cm^{-1} are strong evidence of the existence of an In(III)-nitrato complex, presumably $[In(OH_2)_5ONO_2]^{2+}$. Approximately 60% of the indium is coordinated to NO_3^- in the stock solution. Upon dilution the thermodynamically weak, inner-sphere nitrato complex disappears to form an outer-sphere complex, $[In(OH_2)_6NO_3]^{2+}$ and/or free nitrate. The situation in a concentrated $In(NO_3)_3$ solution is comparable to the situation in a concentrated $Fe(NO_3)_3$ solution,[45] where the nitrato complex formation is also weak.

3.5 Aqueous $In_2(SO_4)_3$ solutions

3.5.1 Raman spectra. A concentration profile of the isotropic Raman spectra of four aqueous $In_2(SO_4)_3$ solutions, 1.659, 0.627, 0.237, and 0.099 mol l^{-1} at 23 °C are presented in Fig. 7a (50–800 cm^{-1}) and in Fig. 7b (800–1300 cm^{-1}). The Raman data are presented in Table S3.‡ The Raman spectra of the $In_2(SO_4)_3$ solutions reveal, through comparison with the modes of "free sulfate" (in $(NH_4)_2SO_4$ solutions), that the sulfate penetrates the first hydration sphere of In^{3+}. All the expected features, which indicate sulfate ion pairing, can be observed in the indium sulfate spectra. The shift of the sulfate due to ligated sulfate, the appearance of a In(III)-OSO_3^{2-} ligand mode at 262 cm^{-1} and down shift of $\nu_1(InO_6)$ from 487 cm^{-1} in the unperturbed state to 475 cm^{-1} and the occurrence of a broad shoulder at *ca.* 430 cm^{-1}. Furthermore, two modes at 430 cm^{-1} and 646 cm^{-1} are observed in the isotropic spectrum. These modes stem from the ligated sulfate. The $\nu_1(SO_4^{2-})$ mode of the unligated sulfate overlaps with the mode of the ligated sulfate of the indium sulfato complex,

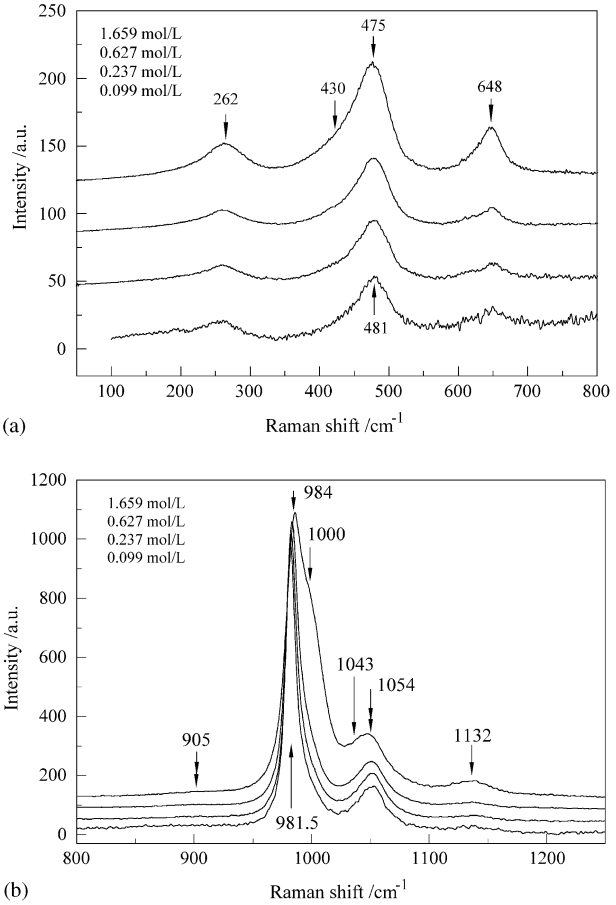

Fig. 7 (a) Concentration profile of the isotropic Raman spectra of aqueous $In_2(SO_4)_3$ solutions (1.659, 0.627, 0.237, and 0.099 mol l^{-1}) at 23 °C in the frequency range from 50 to 800 cm^{-1}. The band maxima are denoted. (b) Concentration profile of the isotropic Raman spectra of aqueous $In_2(SO_4)_3$ solutions (1.659, 0.627, 0.237, and 0.099 mol l^{-1}) at 23 °C in the frequency range from 800 to 1300 cm^{-1}. The band maxima of the sulfate modes (free and ligated) are denoted by arrows and the modes of the hydrogen sulfate are denoted by double headed arrows.

$[In(OH_2)_{6-x}(OSO_3)_x]^{+3-2x}$ at 1000 cm^{-1} resulting in a peak maximum at *ca.* 984.5 cm^{-1}. New polarized modes at 1043 cm^{-1}, 1132 cm^{-1}, and 1205 cm^{-1} are also assigned to ligated sulfate.

The "free" sulfate, which can be observed in the spectra of $(NH_4)_2SO_4$ solution, was discussed by Rudolph and co-workers.[18,46] The spectrum of aqueous $(NH_4)_2SO_4$-solutions shows the "free", undistorted SO_4^{2-} ion (T_d-symmetry), and the nine modes of internal vibrations having the representation Γ_{vib} (T_d) = $a_1 + e + 2f_2$. The $\nu_1(a_1)$-SO_4^{2-} mode at 981.4 cm^{-1} is totally polarized ($\rho = 0.006$), whereas $\nu_3(f_2)$-SO_4^{2-}, centred at 1110 cm^{-1}, and the deformation modes $\nu_4(f_2)$-SO_4^{2-} at 617 cm^{-1} and $\nu_2(e)$-SO_4^{2-} at 452 cm^{-1}, are depolarised. The frequency at 1000 cm^{-1} (see Fig. 8) represents the sulfato complex. The sulfato complex formation may be written according to eqn. (8):

$$In^{3+}(H_2O)_6 \cdot SO_4^{2-} \leftrightharpoons In^{3+}(H_2O)_5OSO_3^{2-} + H_2O \quad (8)$$

Reaction (8) is an endothermic process (increase in aqua-indium(III)sulfato complex with enhancing temperature). The broad weak mode at 905 cm^{-1} and the mode at 1054 cm^{-1} have to be assigned to HSO_4^-, the hydrolysis product [*cf.* vibrational data on HSO_4^- in ref. 19].

The hydrolysis of In^{3+} becomes detectable at 23 °C and a steady increase of the hydrolysis of $[In(OH_2)_6^{3+}]$ is observable with increasing temperature. With temperature decrease the opposite is true and both the hydrolysis is diminished as well as

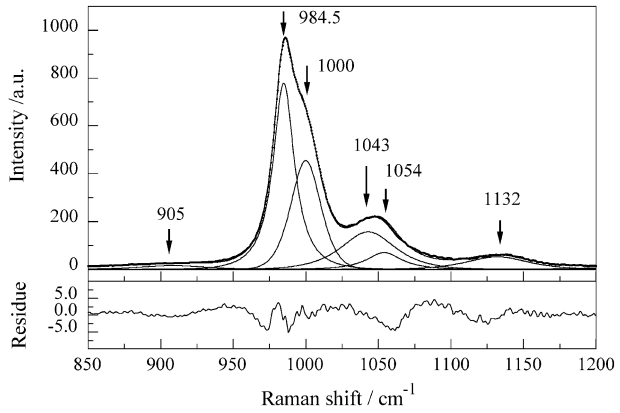

Fig. 8 The isotropic Raman profile, the sum curve and the component bands of the band fit for the 1.659 mol l^{-1} aqueous $In_2(SO_4)_3$ solution at 23 °C. The frequency range comprises 850–1200 cm^{-1}. The very weak mode at 1205 cm^{-1} was omitted for clarity. For the numerical band fit results see Table 4.

the degree of sulfato complex formation. Fig. 9 presents the temperature profile of the isotropic Raman spectrum of a 0.627 mol l^{-1} $In_2(SO_4)_3$ solution at 23 and 0 °C and shows the two effects: decrease in ligated sulfate (mode at 1000 cm^{-1}) and the decrease in hydrolysis and therefore in hydrogen sulfate concentration. The corresponding band fit results are presented in Table S4.‡

The following quantitative considerations can be made. The two modes at *ca.* 905 cm^{-1} and at 1054 cm^{-1} are assigned to the hydrolysis product HSO_4^- (*cf.* ref. 10) and the slightly temperature dependent mode at 983 cm^{-1} is assigned to unperturbed sulfate and sulfate in the solvent separated ion pair. The modes at 1000, 1044, 1132 and 1206 have to be assigned to ligated sulfate (complexed to In^{3+}). The mode at 1044 cm^{-1} is severely overlapped with ν_1 HSO_4^- and its origin is less precise. However, from earlier Raman studies on aqueous HSO_4^- solutions[10] we know that the ratio of $\nu_2(HSO_4^-)$ to $\nu_1(HSO_4^-)$ is 1 : 2.65 and this is achieved in our band fits (Table S4).‡ Consequently, the intensity of mode at 1044 cm^{-1} has to stem from ligated sulfate and not from $\nu_1(HSO_4^-)$. It should be pointed out that the contribution of $\nu_1(HSO_4^-)$ is already a bit overestimated (the actual mole ratio is 1 : 2.75). From the above given quantitative results we can estimate the degree of sulfato complex formation in aqueous In^{3+} sulfate solutions. The degree of sulfato complex formation is clearly diminished at 0 °C compared to the solution at 23 °C. The degree of complex formation of an 0.627 mol l^{-1} In^{3+}-sulfate solution at 0 °C is 0.14, at 23 °C is 0.22, and at 50 °C, it rises to

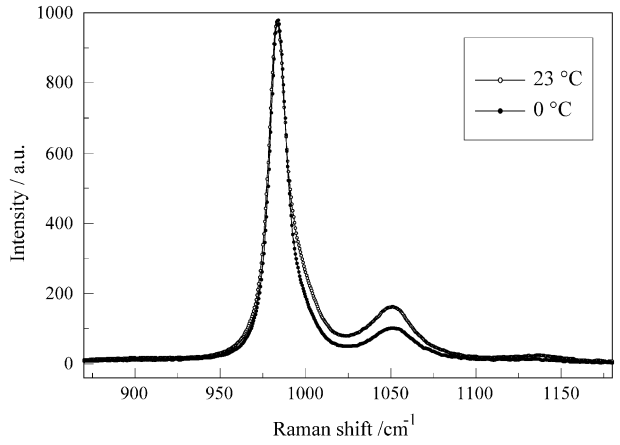

Fig. 9 The isotropic Raman profiles, the sum curve and the component bands of the band fit for a 0.627 mol l^{-1} aqueous $In_2(SO_4)_3$ solution at 23 °C and at 0 °C. The frequency range comprises 850–1200 cm^{-1}. For the results of the numerical band fit see Table 5.

0.29. Clearly, the sulfato complex formation is endothermic, a feature shared with the other group 13 cations Al^{3+} [1] and Ga^{3+}.[2,40] The degree of sulfato complex formation at 23 °C as a function of concentration is: 0.56 (1.659 mol l^{-1}); 0.22 (0.627 mol l^{-1}); 0.17 (0.237 mol l^{-1}), 0.15 (0.099 mol l^{-1}), and 0.12 (0.033 mol l^{-1}). It is noteworthy that even at a concentration of 0.033 mol l^{-1}, the sulfato complex formation persists (spectrum not shown).

The hydrogen sulfate ion is formed as a result of the hydrolysis of $[In(OH_2)_6^{3+}]$:

$$[In(OH_2)_6]^{3+} + H_2O \leftrightharpoons [In(OH_2)_5(OH)]^{2+} + H_3O^+ \quad (9)$$

which is coupled with the sulfate ionization reaction:

$$H_3O^+ + SO_4^{2-} \leftrightharpoons HSO_4^- + H_2O \quad (10)$$

As a result, the degree of hydrolysis influences the equilibrium concentrations of HSO_4^- and "free" SO_4^{2-}. In other words, sulfate acts as a probe to detect the hydrolysis of indium(III) by forming hydrogen sulfate.

At temperatures above 100 °C a basic indium sulfate (BIS) precipitates from the stock solution. This phenomenon also occurs at room temperature, if the indium sulfate stock solution is diluted below 0.005 mol l^{-1}. The stoichiometry of the solid product was determined (mole ratio In : sulfate = 1 : 1) and X-ray diffraction data showed that the salt is $In(OH)SO_4$.[47]

3.5.2 115-In NMR spectra. We have studied the temperature profile of a 1.659 M In(III)-sulfate solution from 21.4 °C to −20 °C. The data are presented in Table 2. The experimental setup was chosen because it was hoped to resolve two 115-In resonance peaks reflecting the indium ligated with sulfate (bound In(III)) and the free, the monomeric form, $[In(OH_2)_6^{3+}]$. We should expect one peak positioned at 0 ppm representing the hexaaqua indium complex ion and the other upfield for the In^{3+} sulfate complex. (The situation in Al- and Ga-sulfate solutions is comparable to this one).[41] However, the 115-In NMR spectrum of the 1.659 mol l^{-1} (1.95 molal) $In_2(SO_4)_3$ solution as a function of temperature contains only one resonance signal at −70 ppm. The very fast water exchange causes the two resonance signals (hexaaquaindium(III) and the indium(III) sulfato complex) to coalesce. This is consistent with recent results by Merbach and co-workers who found a water exchange rate for $k_1 \geq 1 \times 10^7$ s^{-1} at 25 °C.[30] From the Raman data it follows that at 23 °C *ca.* 60% of all In^{3+} exists in the form of a sulfato complex. Because of the very fast exchange only one resonance signal at −70 ppm was observed. Decreasing temperature resulted in a downfield shift of the resonance signal that means less negative ppm values as a result of the decreasing of the amount of the indium(III)–sulfato complex. It is noteworthy that for a 1.65 mol l^{-1} $In(ClO_4)_3$ solution the indium resonance signal is at 0 ppm and does not shift with temperature and the half width of the resonance signal is much smaller compared with the In(III)-sulfate solution. (The half width of the resonance signal is of course also a function of viscosity and the quadrupole moment. The viscosity increases with a decrease in temperature and also

Table 2 Results of the 115 In NMR temperature dependence of a 1.659 mol l^{-1} $In_2(SO_4)_3$ solution

Temperature/°C	Peak frequency/Hz	Half width/Hz	Peak position/ppm	Half width/ppm
−25	−1194	26,245	−18.20	396.93
−10	−4319	11,175	−65.32	169.01
0.0	−4390	8932	−66.39	135.09
9.7	−4731	7682	−71.55	116.18
21.4	−5119	6526	−77.42	98.67

the In^{3+} environment changes from less than octahedral in the indium(III) sulfato complex to octahedral symmetry for the hexaaquaindium (III) cation).

The observed resonance signal is due to an inner-sphere indium–sulfato complex exchanging rapidly with a hexaaquaindium(III) ion. As the temperature is increased more of the indium is present as the sulfato complex which occurs at higher field, and therefore the averaged peak position moves to higher field. The proportion of the coordinated indium increases linearly from −20 to 21.4 °C.

3.5.3 Speciation in aqueous $In_2(SO_4)_3$ solutions. The replacement of water molecules by weak ligands in the hydration sphere of non-transition metals may be explained by the Eigen and Wilkins mechanism:[48]

$$\begin{array}{c} \text{I} \\ In(OH_2)_6^{3+} + SO_4^{2-} \rightleftharpoons In(OH_2)_6^{3+} \\ \text{II} \\ \cdot SO_4^{2-} \rightleftharpoons (In(OH_2)_5OSO_3)^+ \end{array} \quad (11)$$

The first step in reaction (11) is diffusion controlled and leads to the outer-sphere complex. The second step is rate determining and leads to the inner-sphere complex. For $InSO_4^+$ the thermodynamics and kinetics of the reaction outer-sphere complex ↔ inner-sphere complex may be investigated with the pressure-jump relaxation technique. The following equilibria may be stated (compare also the data for the similar $Ga_2(SO_4)_3$–water system[2]):

$$K_o = [InOH_2SO_4^+]/([In^{3+}] \cdot [SO_4^{2-}]) \quad (12)$$

$$K_i = [InOSO_3^+]/[InOH_2SO_4^+] \quad (13)$$

$$K_a = ([InOSO_3^+] + [InOH_2SO_4^+])/([In^{3+}] \cdot [SO_4^{2-}]) = K_o(1 + K_i). \quad (14)$$

K_o, K_i and K_a are the equilibrium constants for the formation of the outer-sphere complex, the inner-sphere complex and for the overall association, respectively. In square brackets the equilibrium concentrations are denoted. For the overall association constant a value of 1096.5 ($I = 0$) at 25 °C[49] was given and is much bigger than our K_i value according to eqn. (13) is approximately 1.2 at 23 °C. This big difference in the sulfato complex constants reflects simply that the traditional methods such as calorimetry[49] measure the overall association constant which means all 1 : 1 indium sulfato complex species such as $InOSO_3^+$, $In(H_2O)SO_4^+$ *etc.* are detected while Raman spectroscopy detects only the indium sulfato complex species, $InOSO_3^+$ and the "free" sulfate.[1,2,40] A carefully executed dielectric relaxation study, as recently carried out on aqueous $MgSO_4$ solutions[50] should be carried out on the $In_2(SO_4)_3$ solutions to obtain information about the speciation as a function of concentration (contact ion pairs, respectively, indium sulfato complex, outer-sphere complex *etc.*).

4 *Ab initio* results

Hydrated indium(III) ions of the general type $[In(OH_2)_n^{3+}]$, n = 1–6, where all waters are in the first-sphere, denoted as In[n + 0], are considered first. Second, we model the modes of the InO_6 unit of the $[In(OH_2)_6^{3+}]$ cluster and include the results on the much larger cluster, $[In(OH_2)_6(OH_2)_{12}^{3+}]$, containing an explicit second hydration sphere. Addition of 12 water molecules reduces the symmetry of the cluster to T. The energy lowering comes from forming four water trimers in the second hydration sphere on alternate faces of the octahedron (*cf.* results in refs. 1–5).

The symmetries of the mono-through hexaaqua complexes are C_{2v}, D_{2d}, D_3, S_4, C_{2v}, and T_h symmetry, respectively. Structural parameters and thermodynamic data of the clusters under consideration can be obtained from the corresponding author. Schematic presentations of the In–O bond length and the incremental binding enthalpy at 298 K as a function of n, the coordination number, are given in Figs. 10 and 11, respectively. Similar graphs for the OH bond length and the HOH angle are found in Figs. S1 and S2.‡ There have only been scattered reports[30,51] dealing with the hydration of trivalent indium water clusters using *ab initio* calculations. A more thorough exposition is warranted, therefore we present the results of calculations on aquaindium(III) clusters using HF and MP2 calculations in combination with a series of different basis sets (STO-3G to 6-31+G*). For clarity only, the results using the 6-31G* and 6-31+G* basis sets are presented. The use of various effective core potentials gave a range of In–O distances. Those containing minimal basis sets (CEP-4G, LANL2MB) gave short distances, those containing unpolarized split-valence basis sets (SDD, SDDAll, LANL2DZ) gave intermediate distances, and those corresponding to polarized split valence basis sets (CEP-31G* and CEP-121G*) gave the longest distances, close to 6-31G*. Inadequacies in the basis set construction may mask any relativistic effects that might be present. The CEP-31G* results (all atoms) compares very favourably with equivalent calculations in the literature (CEP-31G* on In, 6-31G* on O,H),[30] who also noted that correlation and relativistic effects did not play a significant role for hexaaquaindium.

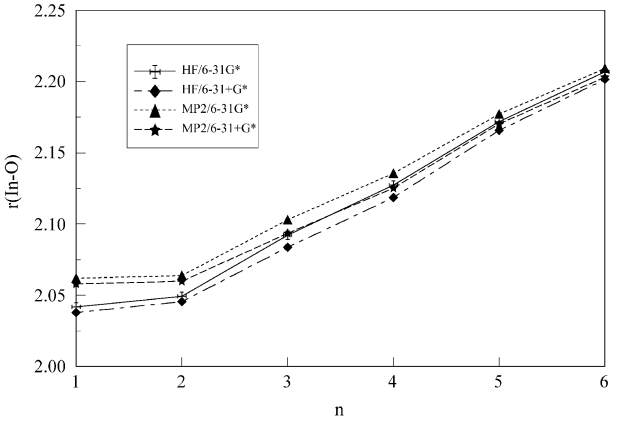

Fig. 10 The In–O bond length (in Å), r(In–O) as a function of the coordination number n for the $In^{3+}(OH_2)_n$ cluster (at HF/6-31G*, HF/6-31+G*, MP2/6-31G* and MP2/6-31+G* levels of theory/basis set).

In Fig. 10 the In–O bond lengths are plotted as a function of the number of water molecules, n, in the first sphere. The bond lengths generally increase with increasing n, a consequence of the steric interactions within the first shell and the concomitant

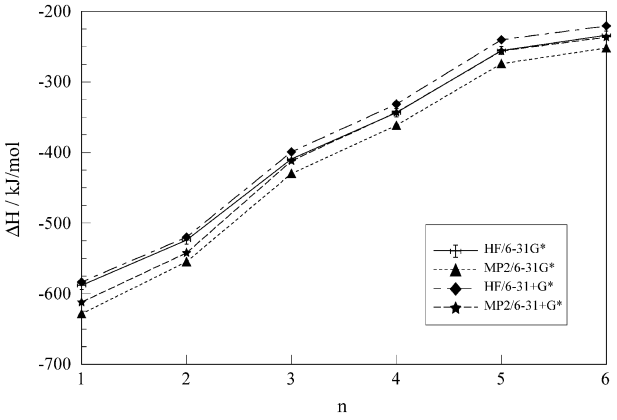

Fig. 11 The incremental binding enthalpy (in kJ mol−1) as a function of the coordination number, n of the $In^{3+}(OH_2)_n$ inner-sphere clusters (at HF/6-31G*, HF/6-31+G*, MP2/6-31G* and MP2/6-31+G* levels of theory/basis set).

Table 3 The In–O symmetric stretching frequency as a function of n, the coordination number, of the aqua In(III) cluster ion for four different basis sets/levels of theory

n	HF/6-31G*	HF/6-31+G*	MP2/6-31G*	MP2/6-31+G*
1	548.8	565.9	520.5	535.8
2	494.8	512.2	476.8	492.8
3	477.5	490.6	466.0	477.4
4	455.4	465.7	447.0	455.8
5	433.8	439.7	429.8	435.8
6	411.9	415.9	410.7	413.7

decrease in indium–water interaction. Figs. S1 and S2 presents the O–H bond length and H–O–H angle as a function of coordination number.‡ The decrease in O–H bond length can be explained by the increase in In–O distance, because the farther away the indium is from the oxygen, the less it can polarize and weaken the O–H bond.

The frequency of the symmetric stretching mode, ν_1 InO_n, as a function of n, the first coordination number, is presented in Table 3. For increasing n, the frequency of the symmetric stretching mode, ν_1 InO_n drops monotonically. It is noteworthy that the frequency $\nu_1(InO_6)$ for $[In(OH_2)_6{}^{3+}]$ cluster is underestimated, as illustrated by both our data and those of Åkesson *et al.*[51] The frequencies of the 51 normal modes of the $[In(OH_2)_6{}^{3+}]$ cluster at the HF/6-31G*, the HF/6-31+G* and the MP2/6-31G* level are listed in Table S5 (supplementary section).‡ For hexaaquaindium(III), the HF and MP2 CEP-31G* and CEP-121G* levels gave similar frequency values as the 6-31G* results, whereas the LAND2DZ, SDD, and SDDAll gave higher frequency values in that order.

The incremental gas phase hydration enthalpies for the reaction: $In^{3+} + nH_2O \rightarrow [In(OH_2)_n{}^{3+}]$ as a function of n are plotted in Fig. 11. As shown in the figure, as the coordination number increases, the hydration enthalpy becomes less exothermic and, thus, the binding energy per water molecule becomes smaller. This behaviour can be attributed to increasing water–water repulsion when the first coordination sphere is subsequently filled. The gas phase binding enthalpy for the hexaaqua cluster (In[6 + 0]) varies from −2295 to −2501 kJ mol^{-1}, depending on the level of theory.

Our *ab initio* calculations on the hexahydrated indium(III) ion (T_h symmetry) are in accord with literature values[30,51] and demonstrate the need for at least a split valence basis set for geometry calculations. The T_h structure of indium(III) hexahydrate is a minima on the potential energy surface and is thus energetically stable. The structural model for this cluster was already presented in Fig. 1. The calculated In–O distance of 2.203 Å (MP2/6-31+G* level) is in fair agreement with the combined EXAFS and LAXS value of 2.131(7) Å, ref. 15 as well as the XRD value of 2.15 Å (ref. 52) for hexahydrated indium(III) in aqueous solution and with the value of 2.112(4) Å in α caesium alum.[17] The structural parameters, energies (hartree) and selected thermodynamic parameters, such as binding energy (at 0 K) and the enthalpy of the cluster formation at 298.15 K were calculated for the $[In(OH_2)_6{}^{3+}]$ cluster and are listed in Table 4.

A recent discussion on the effect of different representations of the solvent medium upon the M-bond length is given in ref. 53 and agrees with our observations of shortening upon explicit incorporation of the second hydration sphere. Although using a self-consistent reaction field approach lengthened the analogous Al–O bond in $[Al(OH_2)_6{}^{3+}]$ by around 0.02 Å, adding 12 explicit water molecules to form a second hydration sphere in both the aluminum and scandium[1] cases had the opposite effect of approximately the same magnitude. The second sphere of the In[6 + 12] cluster (Fig. 12), although having a minor effect on the In–O distance (lowering of *ca.* 0.02 Å), significantly increases the vibrational

Table 4 Optimized geometries, and selected electronic binding energies, $\Delta E_b{}^0$, at 0 K and standard enthalpies $\Delta H_b{}^{298}$ (kJ mol^{-1}) of hexaaqua In(III) cation

	In–O (A)	O–H (A)	H–O–H/°	$-E/E_h$
HF/6-31G*	2.207	0.963	106.49	6191.1081214
MP2/6-31G*	2.209	0.984	106.25	6192.2849235
HF/6-31+G*	2.202	0.962	106.61	6191.1277679
MP2/6-31+G*	2.203	0.986	106.26	6192.3256362
HF/CEP-4G	2.169	1.017	108.29	288.118431
HF/CEP-31G*	2.204	0.965	106.45	288.4624365
MP2/CEP-31G*	2.202	0.989	106.16	289.7542349
HF/CEP-121G*	2.205	0.961	106.68	288.4825902
MP2/CEP-121G*	2.204	0.983	106.56	289.8438253
HF/LANL2MB	2.010	0.977	104.13	451.0655363
HF/LANL2DZ	2.114	0.964	109.24	457.0831732
HF/SDD	2.128	0.964	109.44	457.0883355
HF/SDDAll	2.141	0.963	109.64	102.4152732
MP2/SDDAll	2.163	0.985	109.26	103.2003495

Basis set/level of theory	$\Delta E_b{}^0$	$\Delta H_b{}^{298}$
HF/6-31G*	−2393.82	−2354.79
HF/6-31+G*	−2335.18	−2294.92
MP2/6-31G*	−2537.84	−2500.77
MP2/6-31+G*	−2441.06	(−2402.76)

frequencies of the InO_6 unit and brings them closer to experiment, as shown in Table 5. (The complete frequencies for the 159 normal modes for $[In(OH_2)_{18}{}^{3+}]$ at the HF/6-31G* and HF/6-31+G* level are listed in Table S6 and S7, respectively.‡) Before adding a second hydration sphere, the ν_1 frequency is underestimated compared with the experiment by 50–60 cm^{-1}, as mentioned above. Adding a second hydration sphere results in a significant improvement of the description of the other vibrational frequencies (especially the deformation modes). The results of the CEP-X1G* frequency calculations are similar to that of 6-31G*, whereas the other effective core potentials give higher frequencies (as might be expected from the shorter In–O distances predicted) and any agreement with the experimental value is fortuitous. Compared with the experiment, our best In–O distances are slightly too long and the ν_1 frequency slightly too small. In light of the agreement of other metal ions,[5] the reason for this is not clear. The waters of the second hydration sphere form strong hydrogen bonds between themselves and with the first hydration sphere. The calculated binding enthalpy of this cluster (−3394.59 kJ mol^{-1}; at HF/6-31+G* level) is predominantly due to the electronic component (−3539.74 kJ mol^{-1}; at HF/6-31+G* level)). The single ion hydration enthalpy is −4108.7 kJ mol^{-1} and may be

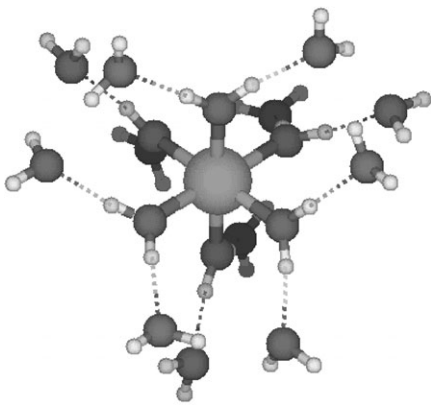

Fig. 12 The structural model of the $[In^{3+}(OH_2)_{18}]$ species (T symmetry) with the first hydration sphere (6 waters) and a complete second hydration sphere (12 waters).

Table 5 Theoretical frequencies (unscaled) of the InO_6 unit for the $[In(OH_2)_6^{3+}]$ cluster and for the $[In(OH_2)_6(OH_2)_{12}^{3+}]$ cluster compared to experimental frequencies of the InO_6 unit from aqueous $In(ClO_4)_3$ solution

$[In(OH_2)_6^{3+}]$			$[In(OH_2)_6(OH_2)_{12}^{3+}]$			
Level of theory/basis set			Level of theory/basis set			
HF/6-31G*	HF/6-31+G*	MP2/6-31G*	HF/6-31G*	HF/6-31+G*	Exp.fr.	Assignment (T)
81	89	74	127	116	—	f_u O–In–O
123	130	105	271	263	306	f_g O–In–O
122	127	116	289	283	—	f_u O–In–O
340	338	347	415	410	410	e_g In–O
400	402	398	460	457	472	f_u In–O
412	416	411	482	487	487	a_g In–O

Remark: Note that in solution the InO_6 unit possesses O_h symmetry (water as point masses seen), the symmetry of the $[In(OH_2)_6^{3+}]$ gas phase cluster is T_h and the symmetry of the $[In(OH_2)_6(OH_2)_{12}^{3+}]$ cluster is T. In cases where two modes of $[In(OH_2)_6(OH_2)_{12}^{3+}]$ correspond, because of mixing with a second-sphere water libration, to a single mode of $[In(OH_2)_6^{3+}]$, the frequency has been averaged.

Table 6 Structural parameters, energy (E_h) and thermodynamic parameters (ΔE_B, binding energy at 0 K, and ΔH^0_{298}, the enthalpy of the cluster formation at 298.15 K) calculated for the $[In(OH_2)_{18}^{3+}]$ cluster denoted In[6 + 12]

Bond length/Å	HF/3-21G	HF/6-31G*	HF/6-31+G*
In–O (first water sphere)	2.1167	2.1781	2.1746
In–O (second water sphere)	4.1090	4.3090	4.3326
O–H (first water sphere)	0.9918	0.9684	0.9690
O–H(A) (second water sphere)	0.9684	0.9526	0.9530
O–H(B) (second water sphere)	0.9820	0.9547	0.9546
HO1···H bond length	1.6505	1.7929	1.8093
Angle Θ/°			
HOH angle (first water sphere)	112.6104	109.3783	109.1686
HOH angle (second water sphere)	111.9978	106.9483	106.9710
Energy/hartree	−7075.7627749	−7103.7294123	−7103.7994795
ΔE_B (0 K)/kJ mol^{-1}	−4896.49	−3686.44	−3539.74
ΔH^-_{298}/kJ mol^{-1}	−4696.73	−3540.66	−3394.59

compared, after corrections, for water vaporization and remaining Born energy. About 83% of the energy is recovered. The structural parameters, energies (hartree) and thermodynamic parameters, calculated for the In[6 + 12] cluster at the HF/6-31G* and HF/6-31+G* level are presented in Table 6.

Recently, a novel S_6 structure of Mg[6 + 12] has been proposed by the Philadelphia Group.[54] This structure is also a local minimum, as is our T structure, which they refer to as PRC. Although their structure is slightly lower in energy, it is not spherical. The degeneracy of the T modes is partially lifted by this structure (a + e modes), but this effect has not been noted experimentally, for which the octahedral model (or its subgroups retaining cubic symmetry, O_h, T_h, and T) suffices. Nonetheless, the structure is of interest and further work is needed to clarify the nature of the second hydration sphere, supplemented by as much experimental data as possible.

5 Conclusions

The medium strong, polarized Raman band assigned to $\nu_1(a_{1g})$ InO_6 mode of the hexaaqua In(III) has been studied in perchlorate over the temperature range from 25 to 75 °C. The position of the $\nu_1(a_{1g})$ InO_6 mode shifts only about 2 cm^{-1} to lower frequencies and broadens about 13 cm^{-1} for a 50 °C temperature increase. Besides the strongly polarized mode at 487 cm^{-1}, two weak depolarized modes at 306 cm^{-1} and 420 cm^{-1} have been assigned to $\nu_2(e_g)$ and $\nu_5(f_{2g})$ of the indium hexaaqua ion. The infrared active mode at 465 cm^{-1} has been assigned to $\nu_3(f_{1u})$. The Raman spectroscopic data suggest that the hexaaquaindium(III) ion is thermodynamically stable in perchlorate solution over the temperature and concentration range measured.

In a concentrated $In(NO_3)_3$ solution, indium exists significantly in the form of both an outer-sphere ion pair, $[In(OH_2)_6^{3+}NO_3^-]$, and an inner-sphere complex, $[In(OH_2)_5ONO_2]^{2+}$. The nitrato complex is thermodynamically weak and disappears completely upon dilution.

Indium sulfate solutions show a different picture and a thermodynamically stable indium(III) sulfato complex could be detected using Raman spectroscopy and 115-In NMR. The formation of the sulfato complex is favoured with increase in temperature and thus entropically driven. At higher temperatures a basic indium(III) sulfate, $In(OH)SO_4$ is formed and was characterised by wet chemical analysis and X-ray diffraction (XRD).

Ab initio geometry optimizations of $[In(OH_2)_n^{3+}]$ clusters, with n = 1–6 have been carried out at the Hartree–Fock and second order Møller-Plesset levels of theory, using various basis sets up to 6-31+G*. The global minimum structure of the hexaaquaindium(III) species corresponds with symmetry T_h. The unscaled vibrational frequencies of the $[In(OH_2)_6^{3+}]$ (In[6 + 0]) were reported, and the vibrational frequencies of the InO_6 unit are lower than the experimental frequencies (*ca.* 20%). The theoretical binding enthalpy for $[In(OH_2)_6^{3+}]$ was calculated and accounts for *ca.* 60% of the experimental single ion hydration enthalpy for In(III). *Ab initio* geometry optimizations and frequency calculations are reported for an $[In(OH_2)_{18}^{3+}]$ (In[6 + 12]) cluster with 6 water molecules in the first sphere and 12 water molecules in the second sphere. The minimum found corresponds with T symmetry. The calculated frequencies of the indium [6 + 12] cluster at the best levels are still underestimated by 10%.

Acknowledgements

The authors would like to thank Dr Ch. R. Jablonski, Department of Chemistry, Memorial University of Newfoundland,

for using the NMR spectrometer and helpful discussions. D.F. would like to thank Gudrun Adam, Institute of Polymer Research Dresden, for preparing and recording the IR spectra. W.W.R. would also like to thank Dr Gert Irmer, TU Mining Academy Freiberg/Saxony and Dr Bob Berno, ARMRC, Halifax, for helpful discussions. The continuing support of NSERC Canada is gratefully acknowledged by C.C.P. Salary support of Human Resources Development Canada to M.R.T. is acknowledged.

References

1 W. W. Rudolph, R. Mason and C. C. Pye, *Phys. Chem. Chem. Phys.*, 2000, **2**, 5030.
2 W. W. Rudolph and C. C. Pye, *Phys. Chem. Chem. Phys.*, 2002 **4**, 4319.
3 W. W. Rudolph, *Z. Phys. Chem.*, 2000, **215**, 221.
4 W. W. Rudolph and C. C. Pye, *J. Phys. Chem. A*, 2000, **104**, 1627.
5 M. R. Michels, T. G. Enright, M. R. Tomney, C. C. Pye and W. W. Rudolph, *Can. J. Anal. Sci. Spectrosc.*, 2003, **48**, 64 and references therein.
6 D. G. Tuck, *Chemistry of Aluminium, Gallium, Indium and Thallium*, ed. A. J. Downs, Blackie Academic and Professional, London, 1993.
7 R. Caminiti, G. Johansson and I. Toth, *Acta Chem. Scand.*, 1986, **A40**, 435.
8 G. Biedermann and D. Ferri, *Acta Chem. Scand.*, 1982, **A36**, 611.
9 P. Brown, J. Ellis and R. N. Sylva, *J. Chem. Soc., Dalton Trans.*, 1982, 1911.
10 M. P. Hanson and R. A. Plane, *Inorg. Chem.*, 1969, **8**, 746.
11 T. Jarv, J. T. Bulmer and D. E. Irish, *J. Phys. Chem.*, 1977, **81**, 649.
12 H. Kanno and J. Hiraishi, *Mem. Natl. Def. Acad. Jpn.*, 1987, **27**, 11.
13 M. A. Marques, M. A. S. Oliveira, J. R. Rodrigues, R. M. Cavagnat and J. Devaure, *J. Chem. Soc., Faraday Trans.*, 1990, **86**, 3883.
14 (*a*) Y. Marcus, *Chem. Rev.*, 1988, **88**, 1475; (*b*) H. Ohtaki and T. Radnai, *Chem. Rev.*, 1993, **93**, 1157; (*c*) D. E. Irish and M. H. Brooker, in *Advances in Infrared and Raman Spectroscopy*, ed. R. J. H. Clark and R. E. Hester, Heyden, London, 1976, vol. 2, p. 212; (*d*) M. H. Brooker, in *The Chemical Physics of Solvation, Part B Spectroscopy of Solvation*, ed. R. R. Dogonadze, E. Kálman, A. A. Kornyshev and J. Ulstrup, Elsevier, Amsterdam, 1986.
15 P. Lindqvist-Reis, A. Muñoz-Páez, S. Diaz-Moreno, S. Pattanaik, I. Persson and M. Sandström, *Inorg. Chem.*, 1998, **37**, 6675.
16 W. E. Harris and B. Kratochvil, *An Introduction to Chemical Analysis*, Saunders College Publishing, Philadelphia, 1981.
17 S. P. Best, J. K. Beattie and R. S. Armstrong, *J. Chem. Soc., Dalton Trans.*, 1984, 2611.
18 W. W. Rudolph, G. Irmer and G. T. Hefter, *Phys. Chem. Chem. Phys.*, 2003, **5**, 5253.
19 W. W. Rudolph, *Z. Phys. Chem.*, 1996, **194**, 73.
20 W. W. Rudolph and G. Irmer, *J. Solution Chem.*, 1994, **23**, 663.
21 (*a*) H, Li-F: W. J. Hehre, R. F. Stewart and J. A. Pople, *J. Chem. Phys.*, 1969, **51**, 2657; (*b*) Rb, Sr, In-Xe: W. J. Pietro, E. S. Blurock, R. F. Hout Jr., W. J. Hehre, D. J. DeFrees and R. F. Stewart, *Inorg. Chem.*, 1981, **20**, 3650.
22 (*a*) H-Ne: J. S. Binkley, J. A. Pople and W. J. Hehre, *J. Am. Chem. Soc.*, 1980, **102**, 939; (*b*) K, Ca, Ga-Kr, Rb, Sr, In-Xe: K. Dobbs and W. J. Hehre, *J. Comput. Chem.*, 1986, **7**, 359.
23 (*a*) C-F 6-31G: W. J. Hehre, R. Ditchfield and J. A. Pople, *J. Chem. Phys.*, 1972, **56**, 2257–2261; (*b*) H, C-F polarization: P. C. Hariharan and J. A. Pople, *Theor. Chim. Acta*, 1973, **28**, 213–222.
24 M. J. Frisch, G. W. Trucks, H. B. Schlegel, P. M. W. Gill, B. G. Johnson, M. W. Wong, J. B. Foresman, M. A. Robb, M. Head-Gordon, E. S. Replogle, R. Gomperts, J. L. Andres, K. Raghavachari, J. S. Binkley, C. Gonzalez, R. L. Martin, D. J. Fox, D. J. Defrees, J. Baker, J. J. P. Stewart and J. A. Pople, *GAUSSIAN 92/DFT, (Revision F.4)*, Gaussian, Inc., Pittsburgh, PA, 1993.
25 S. Huzinaga, J. Andzelm, M. Klobutokski, E. Radio-Andzelm, Y. Sakei and H. Tatewaki, *Gaussian Basis Sets for Molecular Calculations*, Elsevier, Amsterdam, 1984.
26 (*a*) M. J. Frisch, G. W. Trucks, H. B. Schlegel, G. E. Scuseria, M. A. Robb, J. R. Cheeseman, V. G. Zakrzewski, J. A. Montgomery Jr., R. E. Stratmann, J. C. Burant, S. Dapprich, J. M. Millam, A. D. Daniels, K. N. Kudin, M. C. Strain, O. Farkas, J. Tomasi, V. Barone, M. Cossi, R. Cammi, B. Mennucci, C. Pomelli, C. Adamo, S. Clifford, J. Ochterski, G. A. Petersson, P. Y. Ayala, Q. Cui, K. Morokuma, D. K. Malick, A. D. Rabuck, K. Raghavachari, J. B. Foresman, J. Cioslowski, J. V. Ortiz, A. G. Baboul, B. B. Stefanov, G. Liu, A. Liashenko, P. Piskorz, I. Komaromi, R. Gomperts, R. L. Martin, D. J. Fox, T. Keith, M. A. Al-Laham, C. Y. Peng, A. Nanayakkara, M. Challacombe, P. M. W. Gill, B. Johnson, W. Chen, M. W. Wong, J. L. Andres, C. Gonzalez, M. Head-Gordon, E. S. Replogle and J. A. Pople, *GAUSSIAN 98, (Revision A.9)*, Gaussian, Inc., Pittsburgh PA, 1998; (*b*) Web manual: http://www.gaussian.com/g_ur/m_basis_sets.htm.
27 A. Fratiello, R. E. Lee, V. M. Nishida and R. E. Schuster, *J. Chem. Phys.*, 1968, **48**, 3705.
28 G. Johannson, *Adv. Inorg. Chem.*, 1992, **39**, 178.
29 C. F. Base and R. E. Mesmer, *The Hydrolysis of Cations*, John Wiley, New York, 1976.
30 T. Kowall, P. Caravan, H. Bourgeois, L. Helm, F. P. Rotzinger and A. E. Merbach, *J. Am. Chem. Soc.*, 1998, **120**, 6569.
31 I. Nakagawa and T. Shimanouchi, *Spectrochim. Acta*, 1964, **20**, 429.
32 W. Rudolph and S. Schönherr, *Z. Phys. Chem. (Leipzig)*, 1989, **270**, 1121.
33 K. Nakamoto, *Infrared Spectra of Inorganic and Coordination Compounds*, Wiley, New York, 1963.
34 C. I. Ratcliffe and D. E. Irish, *Can. J. Chem.*, 1984, **62**, 1134.
35 R. E. Hester and R. A. Plane, *Inorg. Chem.*, 1964, **3**, 768.
36 H. Kanno, *J. Phys. Chem.*, 1988, **92**, 4232.
37 D. E. Irish and T. Jarv, *Chem. Soc., Faraday Discuss.*, 1978, **64**, 95 and 120.
38 J. K. Beattie and S. P. Best, *Coord. Chem. Rev.*, 1997, **166**, 391.
39 J. Mink, C. Nemeth, L. Hajba, M. Sandström and P. L. Goggin, *J. Mol. Struct.*, 2003, **661–662**, 141.
40 W. W. Rudolph, C. C. Pye and G. Irmer, *J. Raman Specrosc.*, 2002, **33**, 177.
41 T. G. Spiro, *Inorg. Chem.*, 1965, **4**, 731.
42 D. E. Irish, in *Ionic Interactions*, ed. S. Petrucci, Academic Press, New York, 1971, vol. 2, p. 188.
43 (*a*) M. C. R. Symons and D. Waddington, *J. Chem. Soc., Faraday Trans. 2*, 1975, **71**, 22; (*b*) T. J. V. Findlay and M. C. R. Symons, *J. Chem. Soc. Faraday Trans. 2*, 1976, **72**, 820; (*c*) M. R. Waterland, D. Stockwell and A. M. Kelly, *J. Chem. Phys.*, 2001, **114**, 6249.
44 W. W. Rudolph and G. Irmer, *TU Dresden*, 2004, unpublished work.
45 S. K. Sharma, *J. Inorg. Nucl. Chem.*, 1973, **35**, 3831.
46 C. C. Pye and W. W. Rudolph, *J. Phys. Chem. A*, 2001, **105**, 905.
47 W. W. Rudolph and P. Schmidt, *TU Dresden*, 2004, unpublished results.
48 M. Eigen, *Pure Appl. Chem.*, 1963, **6**, 105.
49 R. M. Izatt, D. Eatough, J. J. Christensen and C. H. Bartholomew, *J. Chem. Soc. A*, 1969, 45.
50 R. Buchner, T. Chen and G. Hefter, *J. Phys. Chem. B*, 2004, **108**, 2365.
51 R. Åkesson, L. G. M. Pettersson, M. Sandström and U. Wahlgren, *J. Am. Chem. Soc.*, 1994, **116**, 8691.
52 M. Maeda and H. Ohtaki, *Bull. Chem. Soc. Jpn.*, 1977, **50**, 1893.
53 J. M. Martinez, R. R. Pappalardo, E. Sanchez Marcos, B. Mennucci and J. Tomasi, *J. Phys. Chem. B*, 2002, **106**, 1118.
54 G. D. Markham, J. P. Glusker and C. W. Bock, *J. Phys. Chem. B*, 2002, **106**, 5118.
55 W. W. Rudolph, C. C. Pye and G. Irmer, *Proc. 18th Int. Conf. Raman Spectrosc.*, ed. J. Mink, G. Jalsovszky and G. Keresztury, Wiley, Chichester, 2002.